

Chemical Degradation of a Substituted-Chlorobenzene in an Aqueous Medium Using Palladium Catalysts Tethered by a Hydrophobic Organophosphonic Acid

Yoneda Testuya¹

¹Nihon University, Funabashi, Japan, 274-8501, yoneda.tetsuya@nihon-u.ac.jp

Introduction: In terms of environmental demands for degradation of chlorinated organic compounds including persistent organic pollutants (POPs), hydrodechlorination (HDC) is one of the preferable chemical degradations preventing the formation of toxic oxidative dioxin-like derivatives¹. Recently, organic synthesis for fine chemicals has paid more attention using water solvent²⁻⁵. Correspondingly, an HDC process also in aqueous condition has been reported⁶⁻¹³. Catalytic reaction in water must overcome several weak points: [1] deactivation due to water adsorption on the catalytic surface, and [2] high hydrophobicity of organic substrates. To utilize the catalyst in an aqueous HDC reaction, Dong et.al created two catalysts (magnetic Dendron-like structure⁶ and a metal of framework structure⁷). Hara et al. also made a hydroxyapatite-supported palladium nanoclusters⁸ and its magnetic modification⁹. Subsequently, surface modification covered with organic phase is of importance to solve the weak points. Navon et al. created alumina-supported Pd catalysts coated with hydrophobic silicone polymers¹⁰. Uozumi et al. immobilized Pd nanoparticles in amphiphilic copolymers¹¹. Furthermore, we also found that organosilanes grafting on the silica-support promoted HDC of the aromatic chlorinated compound in water-based solvents¹²⁻¹⁴. While several chlorobenzenes and derivatives have been included in the POPs, other chloro aromatics would be restricted to use in future. Organophosphonic acid has a self-assembling ability, and grafts metal oxide easily; its grafting force is tough in comparison with that of the corresponding organosilanes¹⁵. Herein, we report that the organic/inorganic hybrid catalyst tethered by an organophosphonic acid facilitates to convert a 4-chloroacetophenone to reductive products thereof in a water/ethanol mixture.

Materials and methods: 1. Materials A hydrophobic reactant (4-chloroacetophenone: CLAP) was purified by distillation before reaction. Some products (α -Methyl-benzylalcohol: MBA, acetophenone: AP, ethylbenzene: EB and styrene: ST), solvents (water, ethanol, tetrahydrofuran: THF), a catalyst precursor (palladium (II) tetrammine dichloride monohydrate: Pd(NH₃)₄Cl₂·H₂O) and a tethered reagent (*n*-octadecylphosphonic acid: ODPA) were used without further purification. A silica support removed impurities with hydrochloric acid, washed well with water and dried.

2. Catalyst preparation To estimate the standard performance in the HDC degradation, a bare catalyst (Pd/SiO₂) was obtained through an ion exchange at room temperature (RT), calcination in air at 383 K, and reduction in hydrogen at 423 K. Instead of conventional grafting treatment using organosilanes, the bare catalyst was surface-modified with organophosphonic acid using the “tethering by aggregation and growth” (T-BAG) method¹⁶⁻¹⁹. After soaking in an organophosphonic acid/THF (1 μ mol/L) and spontaneous THF evaporation at RT, the catalyst precursor created an organic/inorganic hybridized catalyst (Pd/SiO₂-ODPA) through heating under argon flowing of 100 mL/min for 24 hours at 413 K.

3. Reaction procedure The palladium on the catalyst (5 mg) in a glass tube was set in a batch reactor, and then activated using reduction under a hydrogen flow of 100 mL/min under 0.5 MPa for 60 min at 413 K. Water (35 mL) was introduced into the glass tube at 373 K. After keeping the temperature, CLAP (2 mmol) in 2:3 (v/v) ethanol/water (5 mL) mixture was introduced using 1 MPa hydrogen, and then allowed starting the HDC reaction. The reaction was examined for 90 min at 373 K.

4. Analysis The products quantitatively analyzed using a gas chromatograph (Shimadzu Co., GC-14B) equipped with a flame ionization detector. Toluene was used as an internal standard. The products were identified using a gas chromatography-mass spectroscopy (Shimadzu Co., GCMS5050QA). The metal loading was measured by an inductively coupled plasma mass atomic emission spectrometry (ICP-AES; SII NanoTechnology Inc., SPS5100). The metal particle was observed by a scanning transmission electron microscopy (STEM) using a

JEM-2100F (JEOL Ltd.). ICP-AES and STEM were performed at the UBE Scientific Analysis Laboratory Inc. Elemental analysis was performed using a JM10 (J-SCIENCE LAB Co., Ltd.). The Brunauer–Emmett–Teller (BET) specific area was obtained using a BELCAT-B (MicrotracBEL Corp.). X-ray photoelectron spectrum (XPS) was obtained from an ESCA 3400 (Shimadzu Co.).

Results and discussion: Table 1 shows the textural characteristics for the bare (Pd/SiO₂) and the hybrid (Pd-SiO₂-ODPA) catalyst. The elemental analysis shows the sum of carbon and hydrogen contents were Pd/SiO₂ (0.1%) and Pd/SiO₂-ODPA (2.6%), meaning that Pd/SiO₂-ODPA has organic substances. Based on the BET specific surface area and the carbon weight percentage, the organic group on the surface of Pd/SiO₂-ODPA is 0.49 groups·nm⁻² using the calculation in the previous report¹². As for metal information, both the catalysts contained a metal loading of 3.6 wt%. Figure 1 depicts particle distribution and STEM images of (A1, A2) the bare and (B1, B2) the grafted catalysts. The STEM in the dark field indicates that the particle sizes (bright points) of Pd/SiO₂ (A2) are smaller than that of Pd/SiO₂-ODPA (B2). The palladium particle ranges of less than 2 nm observed that the particle ratio of Pd/SiO₂ (84%) is higher than that of Pd/SiO₂-ODPA (51%). In contrast, Pd/SiO₂ ratio (0%) in the range of 3-5 nm is lower than that of Pd/SiO₂-ODPA (43%). When observed in other lower magnification, the many metals beyond 10 nm were found in Pd/SiO₂ (14%) in comparison with Pd/SiO₂-ODPA (5%). Though the STEM images seem to show the smaller Pd/SiO₂ particles, the multiple observations prove to show the different size of mean diameters between Pd/SiO₂ (4.5 nm) and Pd/SiO₂-ODPA (3.5 nm). The dispersion calculated from the mean diameters shows the ratio of surface metals per all metals including bulk, where only metal atoms mean 100% dispersion. This tendency indicates a large number of surface metals on metal particles of the Pd/SiO₂-ODPA (31.9%).

Table 1: Characterization of catalysts.

Catalyst	Elemental analysis					BET surface specific area /m ² ·g ⁻¹	Organic group on the support /groups·nm ⁻²	Metal analysis		
	C	H	N	O+P ⁽¹⁾	Ash			Content	STEM diameter	Dispersion
	/wt%							/wt%	/nm	/%
Pd/SiO ₂	0.0	0.1	0.0	4.3	95.7	141	0	3.6	4.5	25.2
Pd/SiO ₂ -ODPA	2.0	0.6	0.0	3.8	93.6	119	0.49	3.6	3.5	31.9

(1): 100-(C+H+N+Ash) %

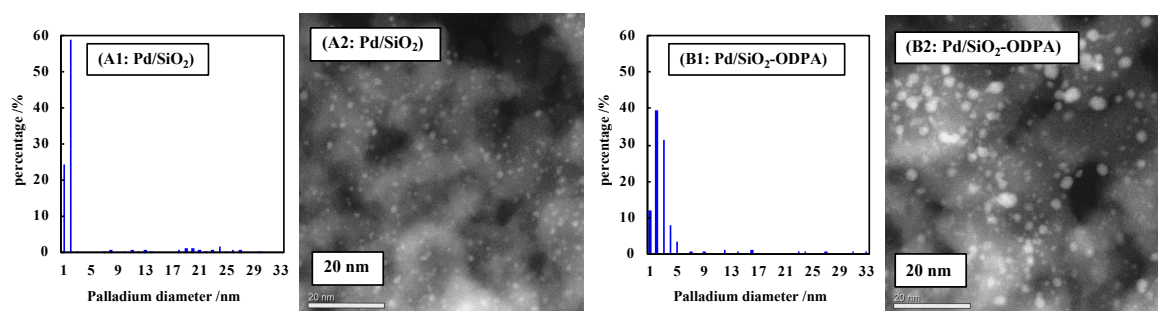


Figure 1: Particle distribution and STEM images of catalysts: (A1, A2) Pd/SiO₂ and (B1, B2) Pd/SiO₂-ODPA.

Figure 2 plots the conversion and product yields for the HDC reaction of CLAP performed over (A) the bare Pd/SiO₂ and (B) Pd/SiO₂-ODPA catalysts in 37:3 (v/v) water/ethanol after 90 min at 373 K. First, the HDC products over the Pd/SiO₂ included acetophenone (AP, 49% yield), α -Methyl-benzylalcohol (MBA, 25% yield), ethylbenzene (EB, 2% yield), styrene (ST, 2% yield), 1-(1-ethoxyethyl)-benzene (ETBA, 1% yield) and 4-chlorostyrene (CS, <1% yield) after 90min, as shown in Figure 2A. Both a reaction conversion and a dechlorination yield mounted to 79.0%. When compared with the bare rhodium catalyst (Rh/SiO₂)¹³, the Pd/SiO₂ showed three differences that [1] Ethylcyclohexane (ECH), acetylcyclohexane (ACH), 1-cyclohexylethanol (CHEL) and 4-chloro- α -methylbenzylalcohol (CMBA) were barely detected, [2] styrene formation occurred, and [3] ETBA was detected. The palladium metal has obviously no hydrogenation of the aromatic ring. As for reaction mechanism, the trace amount of CS in the later periods might contribute to increase ST, while the main reaction scheme observed as follows: the hydrogenolysis of carbon-chlorine bond of CLAP at first step, the hydrogenation of the carbonyl group of AP at second step, and the hydrodeoxygenation of the hydroxy group of MBA at final step. The palladium catalyst also had an undesirable reaction to ETBA formation, meaning condensation between CLAP and ethanol solvent. The previous Pt/SiO₂ catalyst had also the same drawback¹². On the other hand, Figure 2B for the HDC over Pd/SiO₂-ODPA showed that the reaction conversion of 92% and the dechlorination yield of 91% were achieved after 90 min. The products contained AP (46% yield), MBA (33% yield), EB (8% yield), ST (3% yield), ETBA (2% yield) and CS (1% yield) after 90min. In comparison with the dimethyloctadecylsilane-grafted Rh/SiO₂ catalyst¹³, none of ECH, ACH, CHEL, and CMBA were also produced, and the formation of ST, CS and ETBT increased. Thus, the Pd/SiO₂-ODPA also enhanced the HDC pathway from initial hydrodechlorination to next hydrodeoxygenation. That is, reductive cleavage of substituents on the phenyl ring is prior to the hydrogenation phenyl ring in the HDC over the bare and the hybrid catalysts.

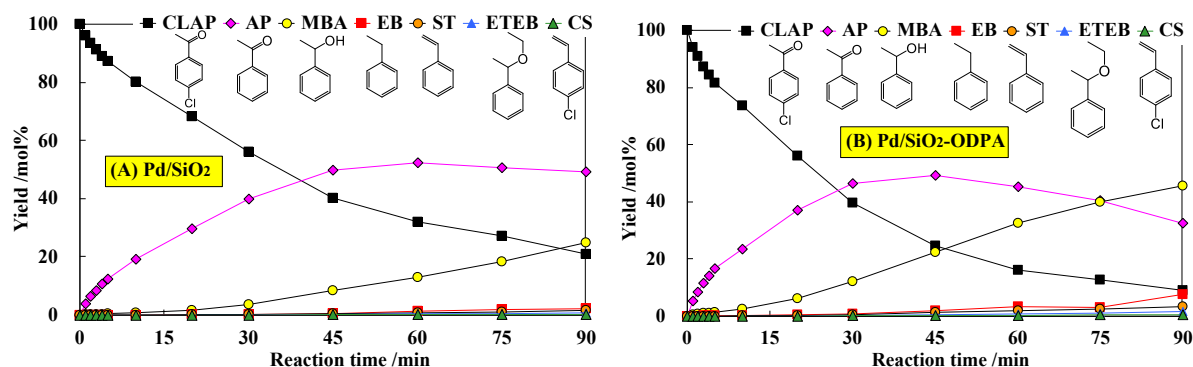


Figure 2: Product yields for the HDC reaction of CLAP in 37:3 (v/v) water/ethanol mixture under 1 MPa hydrogen for 75 min at 373 K: (A) Pd/SiO₂ and (B) Pd/SiO₂-ODPA.

The quantitative comparison about reactivity usually used to the turnover frequency (TOF) which is the effective reaction cycles on the catalyst surface active site (metals) per unit time. TOF on the reaction conversion after 3 min was calculated using the metal dispersions in the textural analyses. The TOF of Pd/SiO₂-ODPA (146 cycles·min⁻¹) was superior to that of Pd/SiO₂ (118 cycles·min⁻¹), indicating that the tethered catalyst is approximately 1.24 times faster than the bare catalyst. Correspondingly, the initial rate at 0 min showed the fact that Pd/SiO₂-ODPA (5.26 mol·min⁻¹) was approximately 1.4 times faster than that of Pd/SiO₂ (3.76 mol·min⁻¹). The improvement depending upon ODPA suggests that the hydrophobicity enhanced the HDC catalyst activity in great volumes of water. A hydrophobic zone on the silica created using the T-BAG technics with ODPA played a significant role that prevents water from adsorbing on the active Pd sites. The previous organosilane-grafted Pt/SiO₂¹² and Rh/SiO₂^{13,14} assisted catalyst activation.

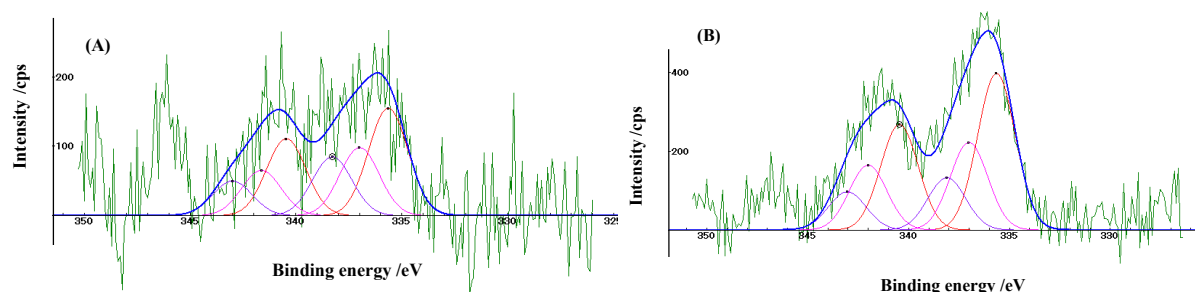


Figure 3: Binding energies in X-ray photoelectron analyses: (A) Pd/SiO₂ and (B) Pd/SiO₂-ODPA.

Figure 3 described XPS results for (A) the bare and (B) the tethered Pd/SiO₂ catalysts. The calibration of binding energy was referenced to the C 2p peak at 285 eV. All deconvolution peaks fitted by Gaussian functions after deleting Shirley-background. The binding energy (BE) peaks of 335 eV and 340 eV were assigned to 3d_{5/2} and 3d_{3/2} of metallic palladium (Pd (0)). Correspondingly, the other deconvoluted BE peaks were observed at first pair of 337 eV and 342 eV (Pd (II), PdO) and the next pair of 338 eV and 343 eV (Pd (IV), PdO₂). These deconvoluted peaks areas for the Pd/SiO₂ were decided to 45%: Pd (0), 30%: Pd (II), and 25%: Pd (IV), respectively. Subsequently, those for the Pd/SiO₂-ODPA were calculated to 53%: Pd (0), 30%: Pd (II), and 18%: Pd (IV). These results indicate the zero-valent metal species on the surface increased after the surface modification using organophosphonic acid. The increased metallic Pd (0) component might assist to promote the HDC reactivity. In summary, the high HDC performance for the tethered Pd/SiO₂-ODPA catalyst stems from [1] its surface affinity gathering hydrophobic chlorobenzene, and [2] high concentration of the zero-valent Pd (0) on the Pd particle surface.

Acknowledgements: This research was supported from Grant-in-Aid for “H28 applied and scientific research (A) of the CST” in Nihon University. I appreciate Dr. Tetsushi Umegaki for his help of the XPS measurement.

References:

- Díaz E., Casas J. A., Mohedano Á. et al. (2009); *Ind. Eng. Chem. Res.* 48 (7): 3351-3358
- Kitanosono T., Zhu L., Liu C., Xu P., Kobayashi S (2015); *J. Am. Chem. Soc.* 137 (49): 15422-15425
- Kitanosono T., Xu P., Isshiki S., Zhu L., Kobayashi, S., et al. (2014); *Chem. Commun.* 50 (66): 9336-9339
- Leung F. K.-C., Ishiwari F., Shoji Y., Nishikawa T., et al. (2017); *ACS Omega* 2 (5):1930- 1937
- Yamada Y. M. A., Ohno A., Sato T., Uozumi Y. (2015); *Chem. Eur. J.* 21 (48): 17269-17273
- Dong Z., Le X., Liu Y., Dong C., Ma J. (2014); *J. Mater. Chem. A* 2 (44): 18775-18785
- Dong Z., Le X., Dong C., Zhang W., Li X., Ma J. (2015); *Appl. Catal. B Environ.* 162: 372-380
- Hara T., Mori K., Oshiba M., Mizugaki T., et al. (2004); *Green Chem.* 6 (10): 507-509
- Hara T., Kaneta T., Mori K., Mitsudome T., et al. (2007); *Green Chem.* 9 (11): 1246-1251
- Navon R., Eldad S., Mackenzie K. et al. (2012); *Appl. Catal. B: Environ.* 119-120: 241-247
- Uozumi Y., Yamada Y. M. A. (2009); *The Chem. Rec.* 9, 51-65
- Yoneda T., Aoyama T., Takido T., Konuma K. (2013); *Appl. Catal. B: Environ.* 142-143, 344-353
- Yoneda T., Aoyama T., Koizumi K., Takido T. (2014); *Chem. Lett.* 43(10): 1603-1606
- Yoneda T. (2016); *Organohalogen Compounds* 78: 1050-1052
- Silverman B. M., Wieghaus K. A., Schwartz J. (2005); *Langmuir* 21 (1): 225-228
- Dubey M., Weidner T., Gamble L. J., Castner D. G. (2010); *Langmuir* 26 (18): 14747-14754
- Vega A., Thissen P., Chabal, Y. J. (2012); *Langmuir*, 28 (21): 8046-8051
- Hanson E. L., Schwartz J., Nickel B. et al. (2003); *J. Am. Chem. Soc.*, 125 (51): 16074-16080
- Hsu C.-W., Liou H.-R., Su, W.-F., Wang (2008); *L. J. Colloid. Interface Sci.* 324 (1-2): 236-239